

## Original Article

**Running Title:** Prognostic Role of miR-551b-3p in Breast Cancer

Received: December 25, 2025; Accepted: February 23, 2026

### Integrated in Silico Analysis Reveals miR-551b-3p as a Potential Tumor Suppressor and Prognostic Biomarker in Breast Cancer

Kübra Su Eda Çelenk\*, MD, Esen Çakmak\*\*, PhD

\*Department of Food Engineering, Graduate School of Natural and Applied Sciences, Kahramanmaraş Sütçü İmam University, Kahramanmaraş, Turkey

\*\* Department of Bioengineering and Sciences, Graduate School of Natural and Applied Sciences, Kahramanmaraş Sütçü İmam University, Kahramanmaraş, Turkey

#### ♦Corresponding Author

Esen Çakmak, PhD

Department of Bioengineering and Sciences,  
Graduate School of Natural and Applied Sciences,  
Kahramanmaraş Sütçü İmam University,  
Kahramanmaraş, Turkey

Email: [esencakmak@ksu.edu.tr](mailto:esencakmak@ksu.edu.tr)

#### Abstract

**Background:** Tumor progression in breast cancer is largely driven by microRNA-mediated post-transcriptional regulatory networks; however, the biological and clinical roles of miR-551b-3p remain insufficiently defined. The present study aimed to characterize the expression profile, molecular interactions, and prognostic relevance of miR-551b-3p in breast cancer via in silico analyses.

**Method:** Designed as an in silico bioinformatic analysis, we assessed miR-551b-3p expression and clinical correlations using the University of Alabama at Birmingham Cancer data analysis portal (UALCAN) and OncoMiR. Associated transcription factors were retrieved from TransmiR v3.0, functional enrichment was performed using the Protein Analysis Through Evolutionary Relationships suite, and survival outcomes were evaluated using Kaplan–Meier Plotter. Statistical significance was evaluated via UALCAN, OncoMiR, and KM-Plotter using t-tests, ANOVA, and log-rank tests, with the threshold set at  $P < 0.05$ .

**Results:** Our analyses revealed a significant downregulation of miR-551b-3p in breast tumor tissues (log-fold change [log-FC] = -1.1,  $P < 0.0001$ ). *TEAD1*, protein tyrosine kinase 2, *SMG1*, *TIMELESS*, *SLC5A3*, and *NUP93* emerged as strong target genes, implicating key pathways involved in proliferation, DNA damage response, and metastatic progression. Furthermore, central transcription factors such as *E2F1*, *ESR1*, *FOXA1*, *CBX3*, and *RAD21* were associated with reduced miR-551b-3p expression. In silico screening identified lncRNAs *AC069281.2/AL359258.1* and *USP9X/TMEM2*-derived circRNAs as potential target-directed microRNA degradation (TDMD) candidates. Clinically, miR-551b-3p downregulation associated with metastasis and unfavorable survival, serving as a supplementary molecular indicator.

**Conclusion:** Collectively, these findings support miR-551b-3p as a potential tumor suppressor and prognostic biomarker in breast cancer, warranting further experimental validation.

**Keywords:** MicroRNAs, Breast neoplasms, Computational biology, Gene expression regulation, Survival analysis

## Introduction

Breast cancer is the most common malignancy among women worldwide and remains a major global health challenge due to its high incidence, mortality, and biological heterogeneity.<sup>1, 2</sup> Although current treatment strategies include surgery, radiotherapy, and systemic therapies, clinical outcomes vary markedly across molecular subtypes. This heterogeneity arises from genomic alterations, diverse signaling pathways within the tumor microenvironment, and subtype-specific biological characteristics. In particular, triple-negative breast cancer exhibits aggressive behavior with limited targeted treatment options and a higher likelihood of recurrence and metastasis compared with other subtypes.<sup>3</sup>

In recent years, non-coding RNAs—especially microRNAs (miRNAs)—have emerged as key regulators of post-transcriptional gene expression and play essential roles in breast cancer biology.<sup>4</sup> miRNAs are short endogenous RNA molecules that fine-tune gene expression by targeting the untranslated regions of mRNAs, thereby inducing degradation or translational repression.<sup>5, 2</sup> Through these mechanisms, miRNAs regulate proliferation, apoptosis, epithelial–mesenchymal transition, invasion, metastatic dissemination, and therapy resistance. Notably, subtype-specific miRNA expression signatures have demonstrated strong potential as diagnostic, prognostic, and treatment-response biomarkers in breast cancer.<sup>6, 7</sup>

Among these regulatory molecules, microRNA-551b-3p (miR-551b-3p) has gained attention due to its context-dependent functions. In breast cancer, elevated nuclear transport of miR-551b-3p via importin-8 (*IPO8*) activates signal transducer and activator of transcription 3 (*STAT3*) signaling and correlates with poor clinical outcomes.<sup>8</sup> Conversely, reduced

expression of miR-551b-3p promotes oncogenic activity in other tumor types, such as lung cancer, by enabling long non-coding RNA (lncRNA) PVT1-mediated increases in cellular proliferation and invasion.<sup>9</sup> Additional studies highlight diverse regulatory axes involving miR-551b-3p, including *Erb-B2* receptor tyrosine kinase 4 (*ERBB4*) suppression in breast cancer<sup>10</sup> and its participation in lncRNA- or autophagy-related pathways in gastric cancer and head and neck carcinoma.<sup>11, 12</sup> Collectively, these findings indicate that miR-551b-3p exerts tumor-suppressive or oncogenic effects depending on the molecular context.

Despite these specific reports, a system-wide view of the miR-551b-3p regulatory landscape and its target interactome in breast cancer remains elusive. In contrast to previous studies that focused on isolated signaling axes, our work integrates high-stringency CLIP-seq binding frequency data, evolutionary conservation metrics, and novel target-directed microRNA degradation (TDMD) scoring. This multi-layered approach aims to systematically identify the miR-551b-3p target network and reconcile its context-dependent roles through large-scale pan-cancer clinical data. By elucidating these biological pathways, we demonstrate that miR-551b-3p acts as a central regulatory node, offering new insights into breast cancer progression and its potential as a supplementary prognostic indicator.

## Materials and Methods

This study was designed as *in silico* bioinformatic analysis based exclusively on publicly available datasets (The Cancer Genome Atlas (TCGA) and Molecular Taxonomy of Breast Cancer International Consortium (METABRIC)); therefore, no pharmacological agents, placebos, or pharmaceutical products were used.

### ***Expression level of miR-551b-3p in breast cancer***

The expression levels of miR-551b-3p in breast cancer tissues and normal controls were assessed using the University of Alabama at Birmingham Cancer data analysis portal (University of Alabama at Birmingham Cancer data analysis portal (UALCAN), <https://ualcan.path.uab.edu>), which provides miRNA-seq and clinical metadata derived from TCGA cohort.<sup>13</sup> Additional expression data, including statistical metrics such as T-test *P*-value, T-test false discovery rate (FDR), tumor Log<sub>2</sub> mean expression, and normal Log<sub>2</sub> mean expression, were retrieved from the OncomiR database (<https://oncomir.org>), a TCGA-based resource for miRNA dysregulation in cancer.<sup>14</sup>

### ***Potential target genes of miR-551b-3p and enrichment analysis in breast cancer***

Potential mRNA targets of miR-551b-3p were obtained from the Encyclopedia of RNA Interactomes (ENCORI) database.<sup>15</sup> High-confidence interactions were selected based on CLIP-supported binding (CLIP-Data  $\geq 5$ ), AGO-paralog evidence, and concordance across multiple prediction algorithms (PITA, miRanda, miRmap, TargetScan, PicTar, microT). For each gene, ENCORI-provided metrics—including TMDB score, TCGA-derived Pearson correlation coefficients, *P*-values, FDR, and prediction-tool support—were collected. Genes passing FDR significance thresholds were retained for downstream functional and pathway enrichment analyses.

The identified target genes were analyzed for gene ontology (GO) and pathway enrichment using the Protein Analysis Through Evolutionary Relationships (PANTHER) classification system.<sup>16</sup> Enrichment analyses included GO biological process (BP), cellular component (CC), and molecular function (MF) categories. Pathway enrichment was assessed using the PANTHER Pathway module, with statistical significance set at  $P < 0.05$ .

### ***Potential lncRNAs and circRNAs of miR-551b-3p in breast cancer***

Potential lncRNA and circular RNA (circRNA) interactors of miR-551b-3p were retrieved from the ENCORI database using AGO-CLIP-supported interactions (AGOExpNumber  $\geq 5$ ) as the primary filtering criterion. Transcription factors (TFs) regulating miR-551b-3p expression were identified through the TransmiR v3.0 database.<sup>17</sup> These datasets were used to construct the extended miRNA-centered regulatory network, including non-coding RNA interactors and upstream transcriptional regulators.

### ***Survival analysis of miR-551b-3p in breast cancer***

Survival analysis of miR-551b-3p in breast cancer was performed using the Kaplan–Meier Plotter (<http://www.kmplot.com>).<sup>18</sup> Overall survival (OS) curves were generated using TCGA breast cancer datasets with the default ‘auto–best cutoff’ option. Hazard ratios (HRs) with 95% confidence intervals and log-rank *p*-values were computed automatically by the KM Plotter statistical module. The maximum follow-up time reached approximately 300 months, based on the TCGA breast cancer survival data used in the Kaplan–Meier analysis. All available cases from the TCGA and METABRIC cohorts were included to maximize statistical power; therefore, a formal sample size calculation was not performed.

### ***Analysis of miR-551b-3p expression in relation to breast cancer clinical parameters***

The association between miR-551b-3p expression and clinical parameters in invasive breast carcinoma was assessed using the OncomiR database.<sup>14</sup> miR-551b-3p expression levels were analyzed in relation to tumor stage and grade by selecting the corresponding miRNA and cancer type. Only associations with statistical significance at  $P < 0.05$  were considered. These analyses provided insights into the potential clinical relevance of miR-551b-3p in breast cancer.

## Results

### **Expression of miR-551b-3p in breast cancer tissues**

In this study, the expression profile of miR-551b-3p in breast cancer was systematically characterized. The analyses demonstrated a significant downregulation of miR-551b-3p in primary breast tumors compared with normal breast tissues (Figure 1a; \*\*\*\* $P < 0.0001$ ), indicating a robust differential expression pattern. A similar trend was observed across breast cancer molecular subtypes (Figure 1b; \*\*\* $P < 0.001$ ), reinforcing the notion that miR-551b-3p loss may be functionally relevant in breast tumorigenesis.

OncomiR analyses further validated this decrease, revealing a statistically significant reduction in tumor samples (two-tailed t-test,  $P = 2.90 \times 10^{-8}$ ; FDR =  $1.10 \times 10^{-7}$ ). The mean  $\log_2$  expression values (1.96 in normal tissues vs. 0.86 in tumor tissues; Table 1) highlight a pronounced downregulation of miR-551b-3p in breast cancer.

### **Target genes of miR-551b-3p in breast cancer**

Potential target genes of miR-551b-3p were identified by integrating multiple high-stringency miRNA–mRNA prediction algorithms with expression correlation analyses (Table 2). The combined analysis revealed a set of candidate genes exhibiting supportive prediction evidence together with statistically significant positive correlations in TCGA-BRCA (The Cancer Genome Atlas Breast Invasive Carcinoma) expression data. To ensure biological relevance, candidates were prioritized based on a stringent intersection of multiple high-stringency parameters.

Among them, *TEAD1*, *SMG1*, and *SLC5A3* emerged as the most prominent potential targets, characterized by a combination of integrative metrics, including high AGO-binding frequency (CLIP-seq), evolutionary conservation, and predictive scores ( $P < 0.01$ , FDR  $< 0.05$ ) (Figure 2).

### **GO and pathway enrichment analysis of target genes**

GO and pathway analyses revealed that the target genes of miR-551b-3p are predominantly associated with cellular processes (31%) and biological regulation (26%). At the MF level, most genes participate in binding (37%) and catalytic activity (32%), while CC analysis indicated that the majority of genes localize to nuclear and cytoplasmic structures (Figure 3).

Pathway analysis highlighted protein tyrosine kinase 2 (*PTK2*) as a central component of Integrin, vascular endothelial growth factor (*VEGF*), and Angiogenesis signaling pathways, suggesting that miR-551b-3p may modulate cell adhesion, migration, and angiogenic processes (Table 3).

### **Prediction of potential lncRNA targets of miR-551b-3p**

miRNA–lncRNA interactions were identified by intersecting AGO-binding regions derived from CLIP-seq data with predicted target sites (Table 4). Based on correlation coefficients and supportive predictive metrics, *AC069281.2* and *AL359258.1* emerged as the most prominent candidate lncRNAs, characterized by consistent negative correlations ( $R = -0.128$ ,  $P < 0.001$ ) and high significance levels (FDR  $< 0.001$ ).

*DLX6-AS1* was identified as a secondary candidate due to its moderate correlation, whereas *LINC00599* exhibited lack of statistical significance ( $P > 0.05$ ). Expression analyses using the UALCAN platform further supported these findings; TCGA data demonstrated a marked upregulation of *AC069281.2* in primary tumor tissues, while *AL359258.1*—nearly undetectable in normal breast tissue—showed a statistically significant increase in tumor samples (Figure 4).

### **Prediction of potential circRNA targets of miR-551b-3p**

CLIP-seq-based integration identified a set of circRNAs with potential binding interactions with miR-551b-3p (Table 5). Since the ENCORI database

reports circRNA candidates using parent gene symbols rather than specific isoform IDs, the names listed in the table (e.g., *TMEM2*, *USP9X*, and *UBC*) represent circRNAs originating from these genomic loci. A joint evaluation using multiple parameters—including AGO-binding frequency, evolutionary conservation, and predictive degradation scores—highlighted *TMEM2*-, *USP9X*-, and *UBC*-derived circRNAs as the most prominent candidates for further analysis.

#### ***The relationship between miR-551b-3p and TFs in breast cancer***

The potential TFs regulated by miR-551b-3p were identified using the TransmiR v3.0 database, revealing TFs involved in proliferation, differentiation, and cancer-related pathways. GEPIA3 analysis indicated that many of these TFs—particularly *E2F1*, *FOXA1*, *ESR1*, *KDM5B*, *CBX3*, and *RAD21*—are markedly upregulated in breast cancer tissues (Table 6).

#### ***Prognostic value of miR-551b-3p in breast cancer patients***

The prognostic significance of miR-551b-3p was evaluated using the Molecular Taxonomy of Breast Cancer International Consortium. OS analysis revealed that patients with low miR-551b-3p expression had significantly poorer survival outcomes compared with those exhibiting high expression levels (HR = 0.64; 95% confidence interval (CI): 0.52–0.79; log-rank  $P = 3.5 \times 10^{-5}$ ; FDR = 1%) (Figure 5).

#### ***Clinical and pathological correlates of miR-551b-3p expression***

Bioinformatic and statistical analyses showed that miR-551b-3p expression is significantly associated with metastasis status (Pathologic M) in breast cancer (analysis of variance (ANOVA)  $P = 1.41 \times 10^{-4}$ ; FDR =  $1.65 \times 10^{-3}$ ; Table 7). In the multivariate survival analysis, however, the association with OS reached a near-significant level ( $P = 0.055$ ) but did not retain statistical significance after FDR correction (FDR = 0.559). Similarly, analyses stratified by tumor size

(Pathologic T) revealed no statistically significant associations following FDR adjustment.

## **Discussion**

In this study, we systematically characterized the expression profile, molecular interactions, and clinical relevance of miR-551b-3p in breast cancer. Our large-scale analysis using TCGA and METABRIC cohorts revealed a significant downregulation of miR-551b-3p across various breast cancer tissues and molecular subtypes, pointing toward a predominant tumor-suppressive loss. Furthermore, we identified key downstream oncogenic target genes and potential upstream non-coding RNA regulators (lncRNAs and circRNAs) associated with this miRNA's depletion. Clinically, we demonstrated that the global loss of miR-551b-3p is robustly associated with disease progression and metastatic status.

Our initial analyses revealed a consistent downregulation of miR-551b-3p across both bulk breast tumor tissues and various molecular subtypes, suggesting a potential tumor-suppressive role in the general breast cancer landscape. While previous literature has indicated that miR-551b-3p might exhibit oncogenic properties in specific contexts—such as through STAT3 activation in triple-negative breast cancer<sup>8</sup>—our large-scale findings point toward a broader trend of depletion. This discrepancy may align with the context-dependent behavior observed in other microRNAs, such as miR-206 and miR-205, which can function either as suppressors or oncogenic drivers depending on the molecular environment.<sup>19, 20</sup> Indeed, the complex regulatory landscape of breast cancer involves both tumor-suppressive miRNAs (e.g., let-7 and miR-139-5p)<sup>21, 22</sup> that are frequently diminished, and oncomiRs (e.g., miR-21 and miR-221/222)<sup>23, 24</sup> that promote invasiveness. Therefore, despite potential subtype-specific oncogenic functions, the widespread reduction of miR-551b-3p

observed in our cohorts suggests that its predominant functional impact may be closely tied to tumor suppression.

Our integrative bioinformatic approach identified several high-confidence downstream targets of miR-551b-3p, including *TEAD1*, *PTK2*, and *NUP93*. Consistent with existing literature, these genes are recognized as central players in cell proliferation and metastatic dissemination.<sup>25, 26, 27,28, 29, 30</sup> Within this context, it is plausible that the escape of *TEAD1*—a key effector of the Hippo–YAP pathway—from miR-551b-3p-mediated repression might potentially drive epithelial–mesenchymal transition and invasion.<sup>26</sup> Interestingly, our analysis also revealed positive correlations between miR-551b-3p and some of these targets, a finding that appears to challenge the classical paradigm of unidirectional miRNA-mediated silencing. This non-canonical pattern could potentially reflect shared upstream regulatory mechanisms or sophisticated feedback loops, wherein target mRNA abundance might influence miRNA stability to maintain cellular homeostasis. Ultimately, these non-canonical relationships underscore the intricate complexity of the miR-551b-3p regulatory network, suggesting that its functions may extend well beyond a simple 'one-way' repression model.

Another layer of regulation identified in our analysis involves potential upstream sponges and degraders, including *TMEM2*- and *USP9X*-derived circRNAs, alongside lncRNAs such as *AC069281.2*. Consistent with emerging literature on competing endogenous RNAs,<sup>31, 32</sup> the high AGO-binding frequency and elevated target-directed microRNA degradation scores of these candidates suggest that they might actively contribute to miR-551b-3p depletion through sequestration or degradation.<sup>15, 33, 34</sup> Furthermore, the evolutionary conservation of these interaction sites supports the potential existence of a preserved regulatory module. Consequently, these findings suggest that

the depletion of miR-551b-3p may not merely be a bystander effect, but could potentially be driven by a highly orchestrated non-coding RNA interactome in malignant tissues.

From a clinical perspective, our findings established a robust association between diminished miR-551b-3p expression and pathologic metastasis status. While miR-551b-3p did not emerge as an independent prognostic factor for overall survival in our multivariate models, its strong correlation with metastatic progression highlights its potential clinical utility. This profile suggests that the prognostic value of miR-551b-3p might partially overlap with established clinical variables, yet it continues to provide valuable biological insights specifically relevant to the metastatic behavior of the tumor. Therefore, rather than serving as a standalone survival predictor, miR-551b-3p could potentially function as an important supplementary biomarker for evaluating metastatic risk.

A major strength of the present study lies in its comprehensive, multi-layered in silico approach, which integrates large-scale clinical cohorts (TCGA and METABRIC), high-stringency RNA-binding data, and evolutionary conservation metrics to systematically characterize the miR-551b-3p network. Despite these methodological strengths, it is important to acknowledge certain limitations. The molecular interactions and prognostic significance identified here are predominantly based on genomic datasets and predictive algorithms. Notably, while the identified Integrin and *VEGF* signaling pathways are influenced by a complex network of competing regulators, our results represent only a specific regulatory facet of this intricate landscape. Furthermore, while high TDMD scores suggest a potential mechanism for miRNA depletion, TDMD remains an emerging concept in RNA biology that requires careful interpretation. Therefore, these computational predictions should be viewed

as robust candidates for further investigation rather than definitively established biochemical pathways. Ultimately, extensive experimental validation through in-vitro assays and in-vivo models will be essential to definitively map the precise biochemical mechanisms and evaluate the therapeutic potential of these identified regulatory nodes in breast cancer.

### Conclusion

The present multi-layered bioinformatic investigation characterizes miR-551b-3p as a significant tumor-suppressive regulator in breast cancer. Our findings demonstrate that the marked downregulation of miR-551b-3p across molecular subtypes is associated with the dysregulation of key oncogenic nodes, including *TEAD1*, *PTK2*, and *NUP93*. The identification of potential upstream inhibitors—specifically lncRNAs *AC069281.2* and *AL359258.1*, alongside high-TDMD-score circRNAs—provides a novel mechanistic framework for the observed miRNA depletion in malignant tissues.

Clinically, although miR-551b-3p did not emerge as an independent prognostic factor for OS, its robust correlation with metastatic status highlights its potential as a supplementary biomarker for metastatic progression. These results suggest that miR-551b-3p primarily modulates the tumor's invasive capacity through Integrin and *VEGF*-associated signaling pathways. While our in-silico data provide strong candidates for therapeutic targeting, further experimental validation remains essential to definitively confirm the biochemical interactions and functional roles of these regulatory axes in breast cancer.

### Data availability

The datasets analyzed during the present study are publicly available in the relevant repositories.

### Ethics approval and consent to participate

Not applicable

### Authors' Contribution

Kübra Su Eda Çelenk and Esen Çakmak contributed equally to the conception and design of the study, data collection, data analysis and interpretation, and manuscript writing and revision. Both authors read and approved the final manuscript and meet the ICMJE authorship criteria.

### Funding

No funding was received for this study.

### Conflict of Interest

None declared.

### References

1. Dvir K, Giordano S, Leone JP. Immunotherapy in breast cancer. *Int J Mol Sci.* 2024;25(14):7517. doi: 10.3390/ijms25147517. PMID: 39062758; PMCID: PMC11276856.
2. Davey MG, Davies M, Lowery AJ, Miller N, Kerin MJ. The role of MicroRNA as clinical biomarkers for breast cancer surgery and treatment. *Int J Mol Sci.* 2021;22(15):8290. doi: 10.3390/ijms22158290. PMID: 34361056; PMCID: PMC8346977.
3. Grimaldi AM, Salvatore M, Incoronato M. miRNA-based therapeutics in breast cancer: A systematic review. *Front Oncol.* 2021;11:668464. doi: 10.3389/fonc.2021.668464. PMID: 34026646; PMCID: PMC8131824.
4. Ismail A, El-Mahdy HA, Abulsoud AI, Sallam AM, Eldeib MG, Elsakka EGE, et al. Beneficial and detrimental aspects of miRNAs as chief players in breast cancer: A comprehensive review. *Int J Biol Macromol.* 2023;224:1541-65. doi: 10.1016/j.ijbiomac.2022.10.241. PMID: 36328268.
5. Çakmak E. Computational and experimental tools of miRNAs in

- cancer. *Middle East J Cancer*. 2020;11(4):381-9. doi: 10.30476/mejc.2020.82239.1069.
6. Jordan-Alejandre E, Campos-Parra AD, Castro-Lopez DL, Silva-Cazares MB. Potential miRNA use as a biomarker: from breast cancer diagnosis to metastasis. *Cells*. 2023;12(4):525. doi: 10.3390/cells12040525. PMID: 36831192; PMCID: PMC9954167.
  7. Ghanbari M, Karari K, Altalebi SAR, Majeed SA, Haghi M. The role of MicroRNAs in breast cancer: diagnostic and therapeutic implications. *Int J Biol Macromol*. 2025;146386. doi: 10.1016/j.ijbiomac.2025.146386. PMID: 40744188.
  8. Parashar D, Geethadevi A, Aure MR, Mishra J, George J, Chen C, et al. miRNA551b-3p activates an oncostatin signaling module for the progression of triple-negative breast cancer. *Cell Rep*. 2019;29(13):4389–406. doi: 10.1016/j.celrep.2019.11.085. PMID: 31875548; PMCID: PMC7380555.
  9. Wang X, Cheng Z, Dai L, Jiang T, Li P, Jia L, et al. LncRNA PVT1 facilitates proliferation, migration and invasion of NSCLC cells via miR-551b/FGFR1 axis. *Onco Targets Ther*. 2021;14:3555–65. doi: 10.2147/OTT.S273794. PMID: 34113122; PMCID: PMC8180410.
  10. Çakmak E, Çelik İS. Diagnostic potential of miR-551b-3p in lung cancer: in vitro and in silico experiments. *Celal Bayar Univ J Sci*. 2025;21(2):125–33. doi: 10.18466/cbayarfbe.1582834.
  11. Yuan H, Chen Z, Bai S, Wei H, Wang Y, Ji R, et al. Molecular mechanisms of lncRNA SMARCC2/miR-551b-3p/TMPRSS4 axis in gastric cancer. *Cancer Lett*. 2018;418(1):84-96. doi: 10.1016/j.canlet.2018.01.032. PMID: 29337109.
  12. Karanam NK, Ding L, Vo DT, Giri U, Yordy JS, Story MD. miR-551a and miR-551b-3p target GLIPR2 and promote tumor growth in high-risk head and neck cancer by modulating autophagy. *Adv Cancer Biol-Metastasis*. 2023;7:100085. doi: 10.1016/j.adcanc.2022.100085.
  13. Chandrashekar DS, Karthikeyan SK, Korla PK, Patel H, Shovon AR, Athar M, et al. UALCAN: An update to the integrated cancer data analysis platform. *Neoplasia*. 2022;25:18–27. doi: 10.1016/j.neo.2022.01.001. PMID: 35078134; PMCID: PMC8788199.
  14. Wong NW, Chen Y, Chen S, Wang X. OncoMiR: an online resource for exploring pan-cancer microRNA dysregulation. *Bioinformatics*. 2018;34(4):713-5. doi: 10.1093/bioinformatics/btx627. PMID: 29028907; PMCID: PMC5860608.
  15. Li JH, Liu S, Zhou H, Qu LH, Yang JH. starBase v2.0: decoding miRNA-ceRNA, miRNA-ncRNA and protein-RNA interaction networks from large-scale CLIP-Seq data. *Nucleic Acids Res*. 2014;42(D1):D92–D97. doi: 10.1093/nar/gkt1248. PMID: 24297251; PMCID: PMC3964941.
  16. Mi H, Muruganujan A, Huang X, Ebert D, Mills C, Guo X, Thomas PD. Protocol update for large-scale genome and gene function analysis with the PANTHER classification system (v.14.0). *Nat Protoc*. 2019;14(3):703-21. doi: 10.1038/s41596-019-0128-8. PMID: 30804569; PMCID: PMC6519457.
  17. Liang M, Zhang C, Yang Y, Cui Q, Zhang J, Cui C. TransmiR v3.0: an updated transcription factor-microRNA regulation database. *Nucleic Acids Res*.

- 2025;53(D1):D318-D323. doi: 10.1093/nar/gkae1081. PMID: 39530226; PMCID: PMC11701595.
18. Posta M, Györffy B. Pathway-level mutational signatures predict breast cancer outcomes and reveal therapeutic targets. *Br J Pharmacol.* 2025;182(23):5734-47. doi: 10.1111/bph.70215. PMID: 41057034.
  19. Quan Y, Huang X, Quan X. Expression of miRNA-206 and miRNA-145 in breast cancer and correlation with prognosis. *Oncol Lett.* 2018;16(5):6638-42. doi: 10.3892/ol.2018.9440. PMID: 30405803; PMCID: PMC6202535.
  20. Petrović N, Todorović L, Nedeljković M, Božović A, Bukumirić Z, Tanić ND, et al. Dual function miR-205 is positively associated with ER and negatively with five-year survival in breast cancer patients. *Pathol Res Pract.* 2022;238:154080. doi: 10.1016/j.prp.2022.154080. PMID: 35994808.
  21. Chirshev E, Oberg KC, Ioffe YJ, Unternaehrer JJ. Let-7 as biomarker, prognostic indicator, and therapy for precision medicine in cancer. *Clin Trans med.* 2019;8(1):24. doi: 10.1186/s40169-019-0240-y. PMID: 31468250; PMCID: PMC6715759.
  22. Sun H, Dai J, Chen M, Chen Q, Xie Q, Zhang W, et al. miR-139-5p was identified as biomarker of different molecular subtypes of breast carcinoma. *Front Oncol.* 2022;12:857714. doi: 10.3389/fonc.2022.857714. PMID: 35433464; PMCID: PMC9009410.
  23. Syed RU, Banu H, Alshammrani A, Alshammari MD, Kadimpati KK, Khalifa AAS, et al. MicroRNA-21 (miR-21) in breast cancer: From apoptosis dysregulation to therapeutic opportunities. *Pathol Res Pract.* 2024;262:155572. doi: 10.1016/j.prp.2024.155572. PMID: 39226804.
  24. Di Martino MT, Arbitrio M, Caracciolo D, Cordua A, Cuomo O, Grillone K, et al. miR-221/222 as biomarkers and targets for therapeutic intervention on cancer and other diseases: A systematic review. *Mol Ther Nucleic Acids.* 2022;27:1191-224. doi: 10.1016/j.omtn.2022.02.005. PMID: 35282417; PMCID: PMC8891816
  25. Akrida I, Makrygianni M, Nikou S, Mulita F, Bravou V, Papadaki H. Hippo pathway effectors YAP, TAZ and TEAD are associated with EMT master regulators ZEB, Snail and with aggressive phenotype in phyllodes breast tumors. *Pathol Res Pract.* 2024;262:155551. doi: 10.1016/j.prp.2024.155551. PMID: 39153238.
  26. González-Alonso P, Zazo S, Martín-Aparicio E, Luque M, Chamizo C, Sanz-Álvarez M, et al. The hippo pathway transducers YAP1/TEAD induce acquired resistance to trastuzumab in HER2-positive breast cancer. *Cancers.* 2020;12(5):1108. doi: 10.3390/cancers12051108. PMID: 32365528; PMCID: PMC7281325.
  27. Yu M, Chen Y, Li X, Yang R, Zhang L, Huangfu L, et al. YAP1 contributes to NSCLC invasion and migration by promoting *SLUG* transcription via the transcription co-factor TEAD. *Cell Death Dis.* 2018;9(5):464. doi: 10.1038/s41419-018-0515-z. PMID: 29700328; PMCID: PMC5920099.
  28. Leeksma AC, Derks IA, Garrick B, Jongejan A, Colombo M, Bloedjes T, et al. *SMG1*, a nonsense-mediated mRNA decay (NMD) regulator, as a candidate therapeutic target in multiple myeloma. *Mol Oncol.*

- 2023;17(2):284-97. doi: 10.1002/1878-0261.13343. PMID: 36400430; PMCID: PMC9892823.
29. Kim M, Hong WC, Kang HW, Kim JH, Lee D, Cheong JH, et al. *SLC5A3* depletion promotes apoptosis by inducing mitochondrial dysfunction and mitophagy in gemcitabine-resistant pancreatic cancer cells. *Cell Death Dis.* 2025;16(1):161. doi: 10.1038/s41419-025-07476-5. PMID: 40055335; PMCID: PMC11889219.
30. Chen Y, Wang W, Fang L, Zhang Z, Deng S. Identification of *PTK2* as an adverse prognostic biomarker in breast cancer by integrated bioinformatics and experimental analyses. *Front Mol Biosci.* 2022;9:984564. doi: 10.3389/fmolb.2022.984564. PMID: 36533074; PMCID: PMC9751198.
31. Kristensen LS, Jakobsen T, Hager H, Kjems J. The emerging roles of circRNAs in cancer and oncology. *Nat Rev Clin Oncol.* 2022;19(3):188-206. doi: 10.1038/s41571-021-00585-y. PMID: 34912049.
32. Chen S, Li X, Guo L, Zhang J, Li L, Wang X, et al. Characterization of the m6A-related lncRNA signature in predicting prognosis and immune response in patients with colon cancer. *J BUON.* 2021;26(5):1931-41. PMID: 34761602.
33. Ren H, Shen X, Xie M, Guo X. Construction of a prognostic score model for breast cancer based on multi-omics analysis of study on bone metastasis. *Transl Cancer Res.* 2024;13(5):2419-36. doi: 10.21037/tcr-23-1881. PMID: 38881940; PMCID: PMC11170530.
34. Singh S, Sinha T, Panda AC. Regulation of microRNA by circular RNA. *Wiley Interdiscip Rev RNA.* 2024;15(1):e1820. doi.org/10.1002/wrna.1820.

Table 1. Statistical comparison of miR-551b-3p expression between normal and tumor breast tissues

miRNA name	T-Test <i>P</i> -value	T-Test FDR	Tumor log <sub>2</sub> mean expression	Normal log <sub>2</sub> mean expression
miR-551b-3p	$2.90 \times 10^{-8}$	$1.10 \times 10^{-7}$	0.86	1.96

FDR: False discovery rate (Benjamini–Hochberg-adjusted I-value)

Table 2. Computationally predicted target genes of miR-551b-3p and their associated statistical parameters in breast cancer tissues compared with normal tissues

Genes	TMDB score	Coefficient-R	<i>P</i> -value	FDR	Prediction tools / Databases
<i>ADGRL1</i>	1.80	-0.06	$3.24 \times 10^{-2}$	$7.27 \times 10^{-2}$	PITA, miRanda, PicTar, TargetScan
<i>CASP2</i>	0.75	0.07	$1.37 \times 10^{-2}$	$3.58 \times 10^{-2}$	PITA, miRmap, miranda
<i>CDC42BPB</i>	1.19	0.03	$2.60 \times 10^{-1}$	$3.74 \times 10^{-1}$	PITA, miRmap
<i>CEMIP2</i>	1.29	0.10	$5.01 \times 10^{-4}$	$2.35 \times 10^{-3}$	PITA, miRmap
<i>COX10</i>	1.56	0.08	$6.37 \times 10^{-3}$	$2.04 \times 10^{-2}$	PITA, miRmap
<i>NCOA4</i>	0.73	0.11	$1.79 \times 10^{-4}$	$1.08 \times 10^{-3}$	PITA, miRmap, miranda
<i>NDELI</i>	0.45	0.03	$3.38 \times 10^{-1}$	$4.55 \times 10^{-1}$	PITA, miRmap, miranda
<i>NDUFA9</i>	0.71	-0.01	$9.37 \times 10^{-1}$	$9.55 \times 10^{-1}$	PITA, miRmap, miranda
<i>NUP93</i>	1.07	0.06	$5.39 \times 10^{-2}$	$1.11 \times 10^{-1}$	PITA, miRmap
<i>PARD6G</i>	0.45	0.07	$1.07 \times 10^{-2}$	$2.95 \times 10^{-2}$	PITA, miRmap, miranda
<i>PDE8A</i>	1.23	0.10	$1.56 \times 10^{-3}$	$5.98 \times 10^{-3}$	PITA, miRmap
<i>PJA1</i>	1.03	0.02	$5.60 \times 10^{-1}$	$6.60 \times 10^{-1}$	PITA, miRmap, microT, miRanda
<i>PTK2</i>	0.98	0.06	$3.76 \times 10^{-2}$	$8.25 \times 10^{-2}$	PITA, miRmap, miranda
<i>SLC5A3</i>	1.04	0.12	$4.54 \times 10^{-5}$	$4.74 \times 10^{-4}$	PITA, miRmap
<i>SMG1</i>	1.31	0.12	$7.12 \times 10^{-5}$	$5.78 \times 10^{-4}$	PITA, miRmap
<i>SMYD4</i>	-1.33	0.02	$5.48 \times 10^{-1}$	$6.58 \times 10^{-1}$	PITA, miRmap
<i>SOWAHC</i>	-0.26	0.04	$1.61 \times 10^{-1}$	$2.63 \times 10^{-1}$	PITA, miRmap, miranda
<i>TEAD1</i>	1.18	0.16	$1.71 \times 10^{-7}$	$7.20 \times 10^{-6}$	PITA, miRmap
<i>TIMELESS</i>	0.79	0.04	$2.33 \times 10^{-1}$	$3.50 \times 10^{-1}$	PITA, miRmap, miranda
<i>UBALD2</i>	0.75	-0.09	$2.18 \times 10^{-3}$	$8.06 \times 10^{-3}$	PITA, miRmap, miranda
<i>ZFP36</i>	0.52	0.02	$4.07 \times 10^{-1}$	$5.14 \times 10^{-1}$	PITA, miRmap, miranda, PicTar
<i>ZNF581</i>	1.17	-0.11	$2.22 \times 10^{-4}$	$1.30 \times 10^{-3}$	PITA, miRmap, miranda

TDMD: Target-directed microRNA degradation score; R: Pearson correlation coefficient; FDR: False discovery rate (Benjamini–Hochberg-corrected *P*-value)

Table 3. GO classification and pathway enrichment of computationally predicted miR-551b-3p target genes in breast cancer tissues

<b>GO category</b>	<b>GO term</b>	<b>Associated genes</b>
Biological process	Biological regulation	<i>PARD6G, TIMELESS, ZFP36, NDEL1, ADGRL1, PTK2, SMG1, ZNF581, TEAD1, PDE8A</i>
	Cellular process	<i>NUP93, PARD6G, TIMELESS, NDUFA9, NDEL1, ADGRL1, CDC42BPB, PTK2, SMG1, COX10, TEAD1, PDE8A</i>
	Developmental process	<i>TEAD1</i>
	Localization	<i>NUP93, NDEL1</i>
	Metabolic process	<i>NUP93, TIMELESS, NDUFA9, PJA1, CDC42BPB, SMG1, COX10</i>
	Multicellular organismal process	<i>TEAD1</i>
	Response to stimulus	<i>TIMELESS, ADGRL1, PTK2, NCOA4, PDE8A, TEAD1</i>
Cellular component	Cellular anatomical entity	<i>PARD6G, TIMELESS, ZFP36, SLC5A3, NDUFA9, NDEL1, ADGRL1, PJA1, CDC42BPB, SMYD4, PTK2, SMG1, NUP93</i>
	Protein-containing complex	<i>NUP93, TIMELESS, NDEL1, TEAD1</i>
Molecular function	Binding	<i>TIMELESS, ZFP36, NDUFA9, NDEL1, SMYD4, ZNF581, TEAD1</i>
	Catalytic activity	<i>PJA1, CDC42BPB, PTK2, SMG1, PDE8A, COX10</i>
	Molecular transducer activity	<i>ADGRL1</i>
	Structural molecule activity	<i>NUP93</i>
	Transcription regulator activity	<i>ZFP36, ZNF581, TEAD1</i>
	Transporter activity	<i>SLC5A3</i>
Pathway	Angiogenesis	<i>PTK2</i>
	CCKR signaling map	<i>PTK2</i>
	Gonadotropin-releasing hormone	<i>PTK2</i>
	Receptor pathway	
	Heme biosynthesis	<i>COX10</i>
	Integrin signaling pathway	<i>PTK2</i>
	VEGF signaling pathway	<i>PTK2</i>

GO: Gene ontology; VEGF: Vascular endothelial growth factor; CCKR: Cholecystokinin receptor

Table 4. Computationally predicted lncRNA candidates regulated by miR-551b-3p and their associated statistical parameters in breast cancer tissues

<b>Genes</b>	<b>TDMD score</b>	<b>Coefficient-R</b>	<b>P-value</b>	<b>FDR</b>
<i>AC069281.2</i>	1.22	-0.13	$2.45 \times 10^{-5}$	$1.23 \times 10^{-4}$
<i>AL359258.1</i>	1.14	-0.13	$2.45 \times 10^{-5}$	$1.23 \times 10^{-4}$
<i>DLX6-AS1</i>	0.15	-0.09	$3.74 \times 10^{-3}$	$1.88 \times 10^{-2}$
<i>LINC00599</i>	0.74	-0.05	$9.06 \times 10^{-2}$	$1.84 \times 10^{-1}$

lncRNA: Long non-coding RNA; TDMD: Target-directed microRNA degradation score; R: Pearson correlation coefficient; FDR: False discovery rate (Benjamini–Hochberg–corrected *P*-value)

Table 5. Computationally predicted circRNA candidates interacting with miR-551b-3p and their associated binding and conservation parameters in breast cancer tissues

<b>Genes</b>	<b>AGOExpNum</b>	<b>RBP</b>	<b>TDMD score</b>	<b>phyloP</b>
<i>RGMB</i>	10	AGO1, AGO2	0.25	3.92
<i>TMEM2</i>	15	AGO1-4, AGO2	1.20	0.30
<i>ANXA11</i>	7	AGO1, AGO2	0.75	-0.03
<i>RPS13</i>	5	AGO1, AGO2	0.51	5.79
<i>COX6A1</i>	13	AGO1, AGO1-4, AGO2	0.46	0.65
<i>UBC</i>	5	AGO1, AGO2	1.18	-1.25
<i>PAFAH1B1</i>	6	AGO2	0.45	6.12
<i>ATP5A1</i>	9	AGO2	0.93	5.04
<i>REXO1</i>	6	AGO1-4, AGO2	0.28	-0.53
<i>hsa_circ_0089761</i>	10	AGO1, AGO2	0.52	2.66
<i>USP9X</i>	5	AGO1-4, AGO2	1.26	5.74

circRNA: Circular RNA; AGOExpNum: Argonaute binding events; RBP: RNA-binding protein; TDMD: Target-directed microRNA degradation score; phyloP: Phylogenetic conservation score across species

Table 6. Differential expression profile of transcription factors predicted to be regulated by miR-551b-3p in breast cancer tissues

<b>TF name</b>	<b>Log<sub>2</sub> FC</b>	<b>P-value</b>	<b>q-value</b>
<i>CBX3</i>	1.00	$1.05 \times 10^{-143}$	$1.70 \times 10^{-143}$
<i>CDYL2</i>	0.68	$8.50 \times 10^{-27}$	$1.91 \times 10^{-27}$
<i>E2F1</i>	2.01	$8.83 \times 10^{-171}$	$2.15 \times 10^{-170}$
<i>ESR1</i>	1.64	$2.67 \times 10^{-23}$	$5.59 \times 10^{-24}$
<i>FOXA1</i>	2.62	$1.40 \times 10^{-58}$	$5.73 \times 10^{-59}$
<i>HDAC2</i>	0.62	$7.51 \times 10^{-40}$	$2.18 \times 10^{-40}$
<i>KDM5B</i>	1.19	$3.81 \times 10^{-99}$	$3.04 \times 10^{-99}$
<i>RAD21</i>	1.02	$2.08 \times 10^{-59}$	$8.63 \times 10^{-60}$
<i>RORC</i>	0.87	$6.92 \times 10^{-23}$	$1.44 \times 10^{-23}$
<i>SMC1A</i>	0.83	$7.54 \times 10^{-37}$	$2.06 \times 10^{-37}$

TF: Transcription factor; Log<sub>2</sub> FC: Log<sub>2</sub> fold change in gene expression between tumor and normal tissues; FDR: False discovery rate (Benjamini–Hochberg-adjusted *P*-value)

Table 7. Association between miR-551b-3p expression and clinical parameters in breast cancer patients

<b>miRNA</b>	<b>Clinical parameter</b>	<b>ANOVA <i>P</i>-value</b>	<b>ANOVA FDR</b>	<b>Multivariate log-rank <i>P</i>-value</b>	<b>Multivariate log-rank FDR</b>
miR-551b-3p	Pathologic M Status	$1.41 \times 10^{-4}$	$1.65 \times 10^{-3}$	$5.51 \times 10^{-2}$	$5.59 \times 10^{-1}$
miR-551b-3p	Pathologic T Status	$4.88 \times 10^{-2}$	$2.00 \times 10^{-1}$	$1.29 \times 10^{-1}$	$6.98 \times 10^{-1}$

Log-rank analysis was performed using a multivariate Cox proportional hazards model. ANOVA: Analysis of variance; FDR: False discovery rate (Benjamini–Hochberg-adjusted *P*-value); BRCA: Breast invasive carcinoma

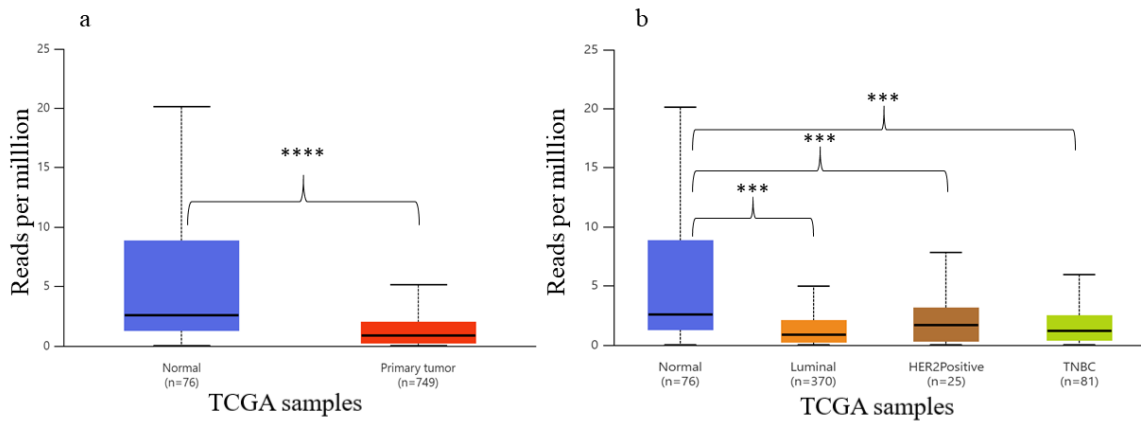


Figure 1. Differential expression of miR-551b-3p in breast cancer; (a) miR-551b-3p expression levels in normal and primary tumor tissues. (b) miR-551b-3p expression levels across different breast cancer molecular subtypes and normal tissues

\*\*\*\* $P < 0.0001$  and \*\*\* $P < 0.001$  indicate statistically significant differences. TCGA: The Cancer Genome Atlas; TNBC: Triple-negative breast cancer; HER2: Human epidermal growth factor receptor 2

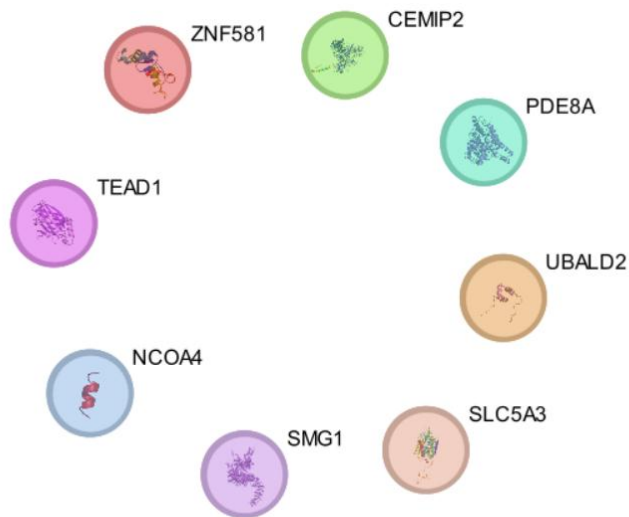


Figure 2. Significantly correlated predicted target genes of miR-551b-3p in breast cancer samples

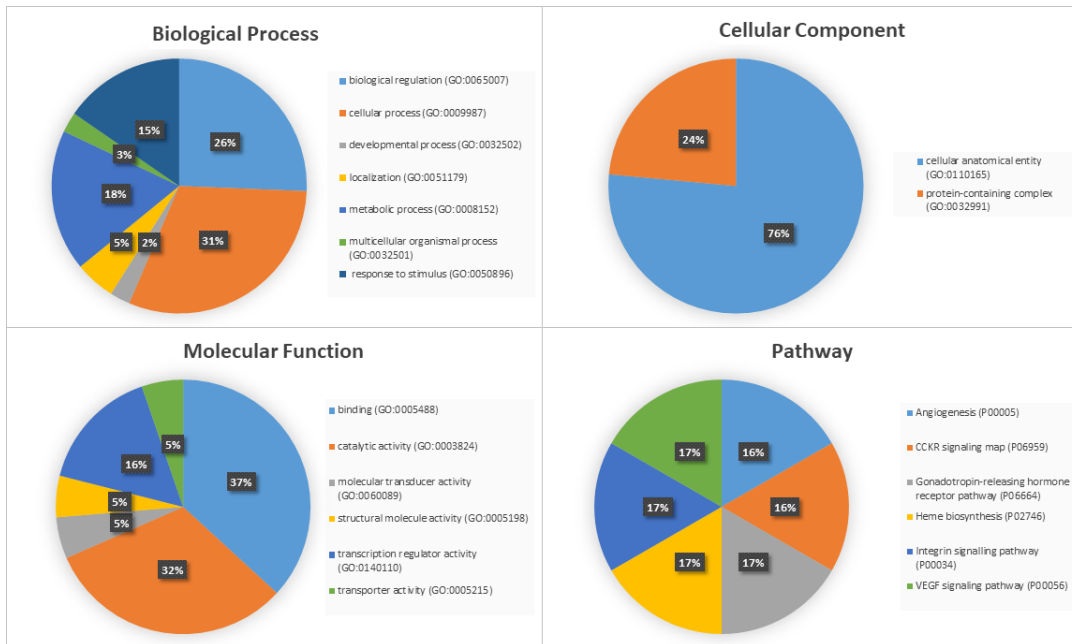


Figure 3. GO and pathway enrichment analysis of predicted miR-551b-3p target genes in breast cancer.

GO: Gene ontology; KEGG: Kyoto Encyclopedia of Genes and Genomes; VEGF: Vascular endothelial growth factor; CCKR: Cholecystokinin receptor

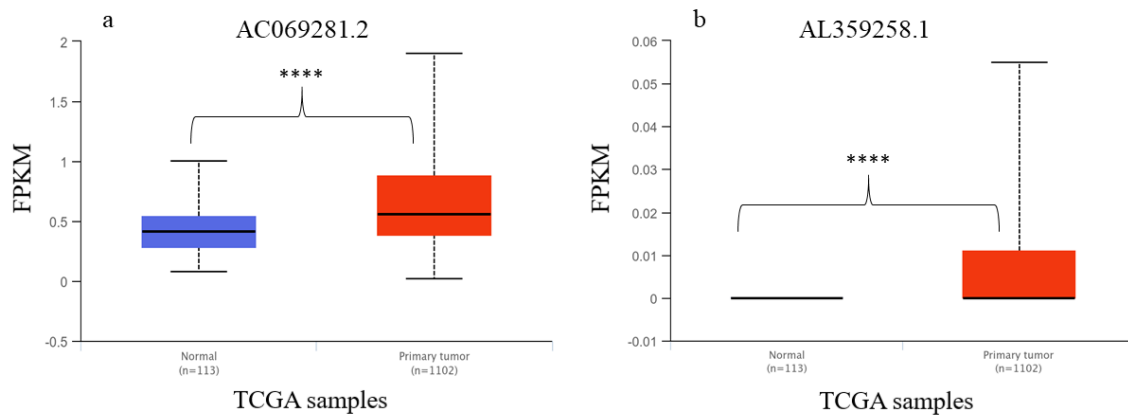


Figure 4. Differential expression of lncRNAs between normal and breast cancer tissues; (a) The expression levels of *AC069281.2*. (b) The expression levels of *AL359258.1*

\*\*\*\* $P < 0.0001$ . TCGA: The Cancer Genome Atlas; FPKM: Fragments per kilobase of transcript per million mapped reads; lncRNA: Long non-coding RNA

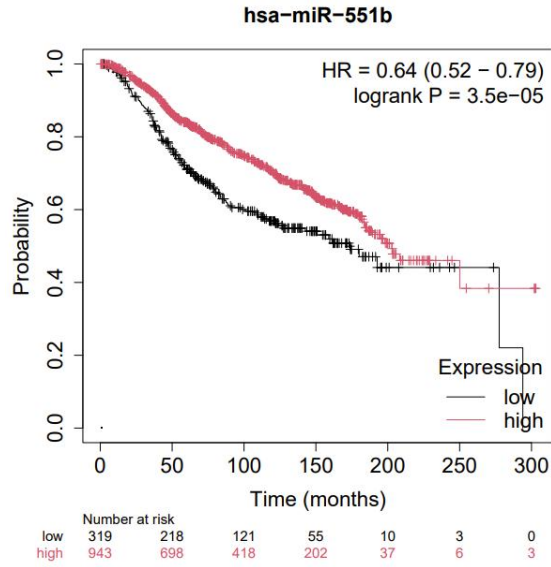


Figure 5. Overall survival analysis of breast cancer patients stratified by miR-551b-3p expression levels

HR: Hazard ratio; CI: Confidence interval